Available online at www.ijournalse.org

Emerging Science Journal

(ISSN: 2610-9182)

Vol. 9, No. 1, February, 2025

A Comparative Study of Material and Structural Configurations in Piezoelectric Energy Harvesting

Fahmidul Huq Syed [1], Li Wah Thong [1*], Mirza Farrukh Baig [2], Yee Kit Chan [1], M. N. Ervina Efzan [2]

[1] *Faculty of Engineering and Technology, Multimedia University, Bukit Beruang, 75450 Malacca, Malaysia.*

[2] *Centre for Manufacturing and Environmental Sustainability, Multimedia University, Bukit Beruang, 75450 Malacca, Malaysia.*

Abstract

The objective of this study is to evaluate the energy harvesting performance of piezoelectric cantilever beams using three configurations—unimorph, bimorph, and stack—with two piezoelectric materials, PZT-5A and PVDF. The methodology involved a detailed analysis of voltage, mechanical power, and electrical power outputs across varying frequencies and load resistances. Experiments were conducted at the resonance frequencies of each beam configuration and material to determine their energy conversion efficiency. The results reveal that PZT-5A significantly outperformed PVDF, with PZT-5A's voltage output being up to 94% higher at resonance. Among the configurations, the bimorph beam with PZT-5A demonstrated the highest energy conversion efficiency, achieving a 50% increase in electrical power output compared to the unimorph configuration and a 9% improvement over the stack configuration. Load resistance analysis also indicated optimal energy harvesting in the range of 10^4 Ω to 10^5 Ω. The novelty of this research lies in its comprehensive comparison of different materials and configurations, highlighting the critical role of structural design and material properties in optimizing piezoelectric energy harvesters for low-power applications. These findings provide valuable insights for improving the efficiency of piezoelectric devices in various practical applications.

Keywords:

Piezoelectric Energy Harvesters;
Vibration Energy;
Cantilever Beam;
PVDF;
PZT-5A.

Article History:

Received:	30	September	2024
Revised:	18	January	2025
Accepted:	21	January	2025
Published:	01	February	2025

1- Introduction

The increasing global demand for sustainable and renewable energy sources has significantly heightened the energy harvesting technologies, particularly piezoelectric energy harvesting. This technology has gained prominence due to its ability to convert mechanical energy into electrical energy, offering a promising solution for powering low-energy devices in various applications [1], such as structural health monitoring [2, 3], wireless sensors [4, 5], and wearable electronics [6–8]. Piezoelectric materials, which generate an electric charge in response to mechanical stress, have become key components in these systems. As technological advancements accelerate, energy consumption has surged, creating an urgent need to shift from finite, environmentally harmful non-renewable energy sources to renewable alternatives [9]. Over the past few decades, researchers have increasingly focused on harnessing renewable energy sources, such as heat, solar, wind, hydro, and vibrations [10, 11]. Among these, vibrations are particularly noteworthy as a substantial natural energy source. Although most vibration sources generate power in milliwatts, their potential to support the growing demand for wearable devices, sensors, and the Internet of Things (IoT) is significant, making piezoelectric energy harvesting a critical area of research and development [12, 13].

* **CONTACT**: lwthong@mmu.edu.my

DOI: http://dx.doi.org/10.28991/ESJ-2025-09-01-019

Previous studies have explored various aspects of piezoelectric energy harvesting, particularly using cantilever beams with tip masses, which have been shown to lower operating frequencies and increase energy output [14]. Over the years, several methods have been investigated to improve performance, including frequency tuning, frequency up-conversion, introducing an S-shaped wavy beam [15], multi-mode dynamic magnifiers [16], and sliding mass techniques [17] to widen the bandwidth and enhance performance. Comparative studies of cantilever beams using piezoelectric materials on steel, copper, and aluminum substrates have revealed that steel and copper outperform aluminum in terms of voltage and power outputs [18]. Other studies have focused on optimizing mechanical and electromechanical designs of piezoelectric systems, emphasizing material selection and structural configurations to improve energy harvesting efficiency in wireless sensor networks [19]. Despite these advancements, a notable gap in the literature persists regarding the optimal selection of materials and cantilever beam designs to maximize energy conversion efficiency, particularly under variable mechanical loading conditions.

Cantilever designs, such as rectangular and trapezoidal, exhibit varying energy harvesting efficiencies, with trapezoidal designs outperforming others at higher resistor values [20]. Innovative structures like auxetic metamaterials further enhance piezoelectric performance by activating multiple modes, achieving voltages as high as 28.2 V [21]. The choice of piezoelectric materials, such as PZT-5H versus PZT-5A, also plays a significant role in power output, with PZT-5H yielding higher results [22]. Lead-free piezoceramics, while gaining attention, demonstrate stable voltage outputs and controllable current densities, which are crucial for practical applications [23]. Studies comparing PZT-5A, PZZN-PLZT, and PVDF in bimorph and unimorph configurations have found that PZT-5A and PZZN-PLZT are superior for energy harvesting, while PVDF is less effective [24]. Despite these advancements in structural and material innovations, challenges remain in achieving consistent output and integrating these technologies into real-world applications, underscoring the need for continued research in this evolving field [25].

Despite these advancements, many studies have focused on optimizing piezoelectric energy harvesting for single-resonant frequencies, which limits their applicability to a narrow range of operational conditions [26–29]. However, piezoelectric energy harvesting still faces significant challenges, as highlighted in Figure 1. The region marked in yellow illustrates the current output of piezoelectric energy harvesters, characterized by a peak at a single frequency, which restricts their usefulness for specific devices and applications. This limitation is especially pronounced in environments where vibration frequencies fluctuate, necessitating broader bandwidth and more consistent output [30, 31].

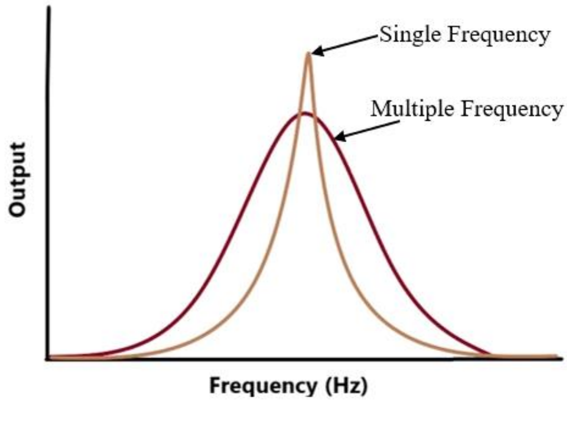

Figure 1. **Limitation of piezoelectric energy harvesting method**

Over the years, extensive research has been conducted to improve the efficiency and applicability of piezoelectric energy harvesting across industrial domains [32]. Despite these advancements, a significant challenge remains in enhancing the bandwidth and overall performance of piezoelectric energy harvesters. Current technology typically produces peak output at a single resonant frequency, limiting its applicability. To achieve broader and more consistent output across multiple frequencies, improvements in the design and materials of piezoelectric energy harvesters are essential.

This study aims to systematically investigate the energy harvesting performance of these three cantilever beam configurations—unimorph, bimorph, and stack—using two piezoelectric materials, PZT-5A and PVDF. The experimental setup includes varying frequencies and load resistances to simulate real-world conditions. By analyzing voltage, mechanical power, and electrical power outputs, the study seeks to identify the optimal material and beam configuration for maximizing energy conversion efficiency under varying conditions. Additionally, the research explores the relationship between power output and load resistance, which is critical for designing adaptable energy harvesting systems capable of operating under different loads. The findings of this research are expected to contribute to the optimization of piezoelectric energy harvesters, improving their efficiency and expanding their applicability in diverse real-world scenarios. By comparing the performance of PZT-5A and PVDF in different structural configurations, this study not only highlights the strengths and limitations of each material and configuration but also provides a comprehensive framework for selecting the most suitable design for specific energy harvesting applications.

This paper is structured as follows: Section 2 outlines the methodology, describing the experimental setup. Section 3 provides the theoretical background and working principles of piezoelectric energy harvesting, focusing on the materials and configurations used in this study. Section 4 details the analytical methods and simulation parameters employed. Section 5 presents the results and discussion, offering a comparative analysis of the performance of PZT-5A and PVDF across unimorph, bimorph, and stack configurations. Lastly, Section 6 concludes the study, summarizing the key findings and offering suggestions for future research to further optimize piezoelectric energy harvesting systems.

2- Research Methodology

In this study, three types of piezoelectric cantilever beams—unimorph, bimorph, and stack—were tested using two piezoelectric materials, PZT-5A and PVDF, to evaluate their energy harvesting performance. The experimental setup involved simulating voltage and power outputs across varying frequencies and load resistances. The vibration frequency was varied between 10 Hz and 300 Hz to reflect real-world low-frequency mechanical loading conditions commonly found in energy harvesting applications such as structural health monitoring and machinery vibrations. The amplitude of oscillations was adjusted between 0.1 mm and 1 mm, simulating different mechanical stress levels. Voltage outputs were captured using a digital oscilloscope, while power output was measured by incorporating a load resistor into the circuit, with power calculated based on the voltage drop across the resistor.

The tests were conducted under ambient temperature conditions (approximately 25°C) to ensure environmental consistency and eliminate temperature-related performance variations. Mechanical loading was further varied by applying different masses to the beams, simulating diverse operational conditions. Voltage, mechanical power, and electrical power were measured for each configuration, and the results were compared to identify the optimal combination of beam structure and material for maximizing energy conversion efficiency. The analysis focused on determining the best-performing system based on output data. The workflow of the study is outlined in Figure 2.

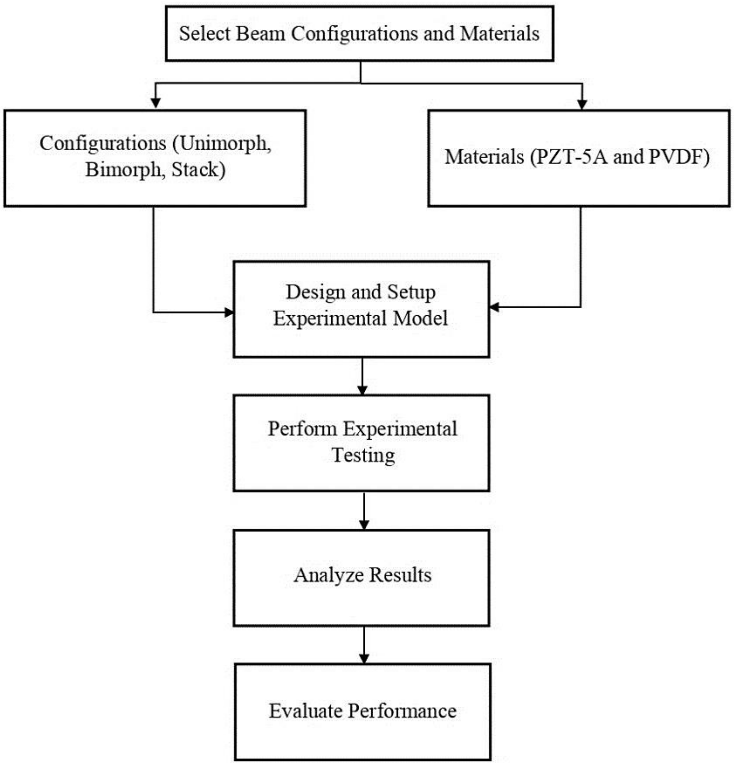

Figure 2. Flowchart of the study

3- Design of Piezoelectric Energy Harvester

3-1- Type of Cantilever Beam

The structural configuration of a piezoelectric device plays a crucial role in its energy harvesting capabilities [33]. These devices are typically configured as unimorph, bimorph, or stack cantilever beams, each offering distinct advantages, as shown in Figure 3. Unimorph configurations, which consist of a single piezoelectric layer bonded to a non-piezoelectric substrate, are simpler to fabricate and integrate. Bimorph configurations, comprising two piezoelectric layers, often yield higher energy outputs due to the increased strain experienced by the material. Stack configurations, involving multiple piezoelectric layers, can further enhance energy output but may introduce additional complexity in device fabrication and load management.

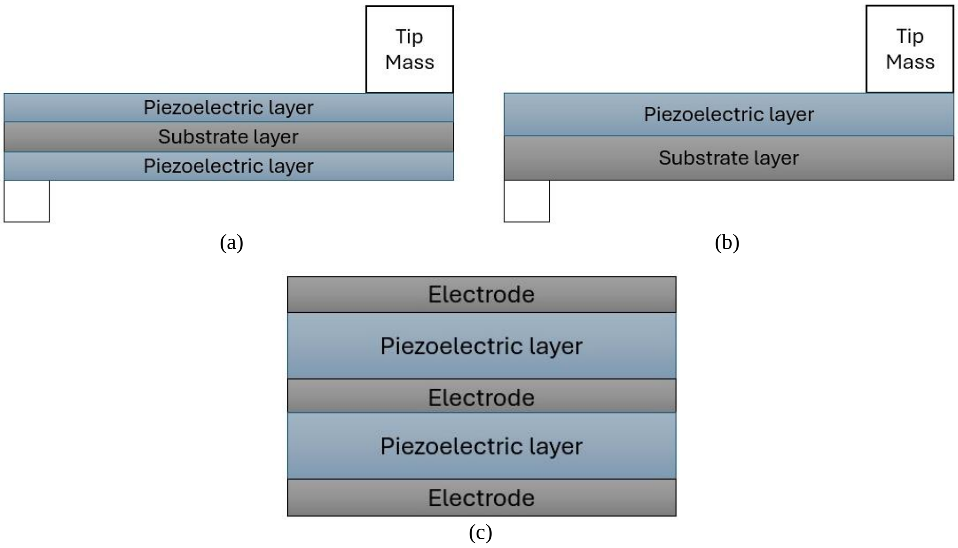

Figure 3. (a) Unimorph (b) Bimorph (c) Stack

3-2- Piezoelectric Materials

The initial discovery of the piezoelectric effect in quartz crystals led to the development of new piezoelectric materials to meet industrial demands. Researchers analyzed the molecular structure of quartz to understand the principles behind piezoelectricity, recognizing that any material with polar bonds and specific lattice symmetry could exhibit these properties. Since then, a variety of organic, synthetic, composite, and ceramic piezoelectric materials have been developed. Inorganic materials, such as lead zirconate titanate (PZT) and barium titanate (BT), have demonstrated strong piezoelectric effects [34], especially when enhanced through processes like poling, with BT recognized for its superior dielectric constant [35, 36]. Although organic materials, like polyvinylidene fluoride polymer (PVDF), discovered in 1969 [37], may not match the piezoelectric performance of their inorganic counterparts, they offer advantages such as durability, flexibility, and cost-effectiveness [38]. To address the limitations of both material types, composite materials have been developed [39, 40], integrating nanosized ceramics within polymer matrices to enhance both performance and flexibility [41]. This study examines the piezoelectric properties of two such materials: PVDF and PZT-5A.

4- Analytical Method

The analytical model is expressed by Euler-Bernoulli's Equation of motion for a single beam piezoelectric harvester with a tip mass [42]:

$$EI\frac{d^4w}{dx^4} + m\frac{dw^2}{dt^2} + c\frac{dw}{dt} + kw + k_t(w - w_t) = F_p + F_e \tag{1}$$

In this context, EI denotes the beam's flexural rigidity, which is the product of Young's modulus (E) and the moment of inertia (I) of the beam. The variable w represents the vertical displacement of the beam in the transverse direction, x indicates the axial position along the beam, and t stands for time. The parameter m signifies the total mass of the beam, including the tip mass, while c is the damping coefficient, and k represents the beam's stiffness coefficient. Additionally, k_t defines the stiffness of the tip mass, w_t is the displacement of the tip mass, and F_p and F_e represent the applied excitation force and the electromechanical force generated by the piezoelectric material, respectively.

Given the two different types of cantilever beams, distinct capacitance formulas apply to each, modified to account for the substrate material. Equation 2 applies to the bimorph cantilever beam, while Equation 3 corresponds to the unimorph cantilever beam.

$$C = \frac{\varepsilon_0\,(\varepsilon_{r,p} \cdot A_p + \varepsilon_{r,s} \cdot A_s)}{d_p + d_s} \tag{2}$$

$$C = \frac{\varepsilon_0\,\varepsilon_r A}{d} \tag{3}$$

In these cases, C stands for capacitance, ε_0 is the vacuum permittivity (approximately $8.854 \times 10^{-12}\ F/m$), and ε_r is the relative permittivity of the piezoelectric material. A represents the effective area of the piezoelectric layer, and d is the separation distance between the piezoelectric layer and the opposing electrode. Additionally, $\varepsilon_{r,p}$ and $\varepsilon_{r,s}$ refer to the relative permittivity of the piezoelectric and substrate materials, respectively. A_p and A_s represent the areas of the piezoelectric and substrate elements, and d_p and d_s are their thicknesses.

The Equations for voltage and electrical power are as follows:

$$V = g \cdot d_{31} \cdot \frac{\Delta p}{\varepsilon_0 \cdot \varepsilon_r \cdot A_{eff}} \tag{4}$$

$$P = 0.5 \cdot C \cdot V^2 \cdot f \tag{5}$$

In Equation 4, V is the voltage output, g is the piezoelectric voltage constant, d_{31} represents the piezoelectric strain constant, and Δp is the mechanical strain induced in the piezoelectric material by external forces. In Equation 5, P denotes the electrical power generated in milliwatts, f indicates the frequency of mechanical excitation. This analytical model has been applied through the finite element method (FEM) to simulate the system and obtain the resulting outputs.

4-1- Simulation Parameters

A 2D representation of a simple cantilever beam was created and analysed by FEM. This paper explores the fundamental principles of a single-beam piezoelectric energy harvester with a tip mass, considering various parameters to evaluate the resulting outputs. Table 1 provides an overview of the key parameters included in this simulation study.

Table 1. Simulation parameters

Parameters	Details
Types of cantilever beam	Unimorph Bimorph Stack
Piezoelectric Materials	Lead Zirconate Titanate-5A (PZT-5A) Polyvinylidene Fluoride Polymer (PVDF)
Proof Mass Material	Aluminium
Resistance	0.5-15 kΩ
Frequency Range (Linear)	0-150 Hz 0-300 Hz

Table 2 illustrates the geometric parameters of the cantilever beam, reflecting the type of setup and the inclusion of the tip mass, while Table 3 displays the properties of the various piezoelectric materials used in the simulation.

Table 2. Simulation parameters

Parameters	Values
Length of the tip mass	4 mm
Height of the tip mass	1.7 mm
Length of cantilever beam	21 mm
Height of the cantilever beam	0.16 mm
Thickness of piezoelectric layer in a bimorph cantilever beam	0.12 mm (0.06/layer)
Thickness of substrate layer in a bimorph cantilever beam	0.04 mm
Thickness of piezoelectric layer in a unimorph cantilever beam	0.08 mm
Thickness of substrate layer in a unimorph cantilever beam	0.08 mm
Thickness of piezoelectric layer in a stack cantilever beam	0.18 mm (0.06/layer)

Table 3. Properties of Piezoelectric Materials

Material	Young's Modulus (GPa)	Density (kg/m^3)	Poisson's ration
Lead Zirconate Titanate-5A	66	7750	0.31
Polyvinylidene Fluoride Polymer (PVDF)	3.8	1780	0.33

These parameters were configured to simulate each cantilever setup using FEM over a frequency range of 0-150 Hz. During the simulation, the thickness of the piezoelectric layer, resistance, and types of piezoelectric materials were varied, while the other conditions remained constant.

5- Results and Discussion

5-1- Validation of Results

To validate the accuracy of the present results, we compared the voltage and electrical power outputs with those reported in the study [43], which examined the performance of piezoelectric energy harvesters under similar experimental conditions. The comparison revealed a strong alignment between our findings and those of [43], particularly regarding voltage levels and power outputs observed across varying frequencies, as demonstrated in Figure 4. This close correlation affirms the reliability of our experimental setup and reinforces the validity of our findings.

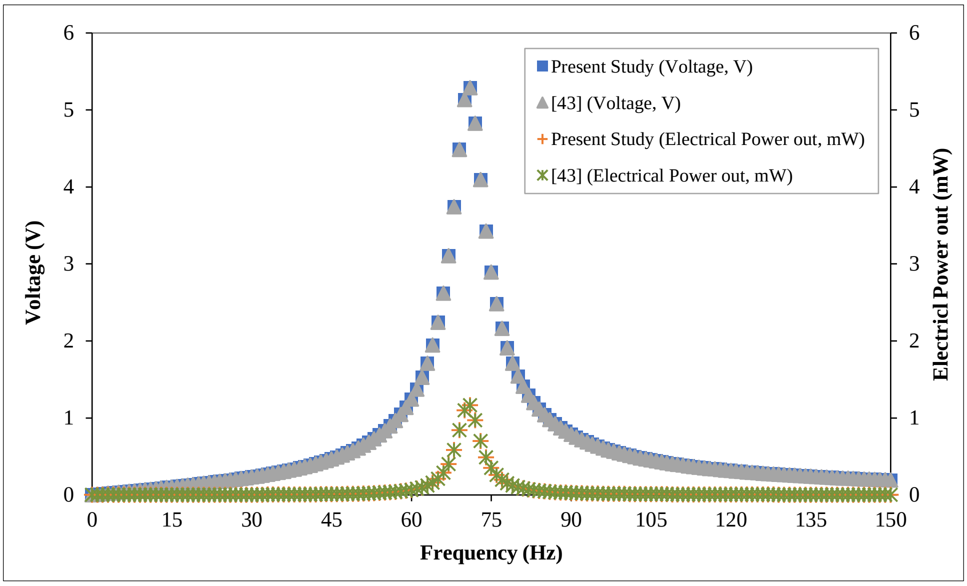

Figure 4. Validation of results

5-2- Types of Cantilever Beam

Figure 5 presents a comparative analysis of the voltage and electrical power output of bimorph and unimorph cantilever beams as functions of frequency. Figure 5-a shows that the bimorph cantilever beam significantly outperforms the unimorph beam. The bimorph beam achieves a peak voltage of approximately 5.13 V at a resonant frequency of 70 Hz, whereas the unimorph beam reaches its maximum voltage output of around 3.67 V at a higher resonant frequency of 90 Hz. This difference highlights the superior performance of the bimorph beam, which not only generates a higher voltage but does so at a lower frequency. Additionally, the bimorph beam maintains a broader frequency response, continuing to produce substantial voltage over a wider frequency range, while the unimorph beam's voltage output is more confined, indicating a narrower effective bandwidth.

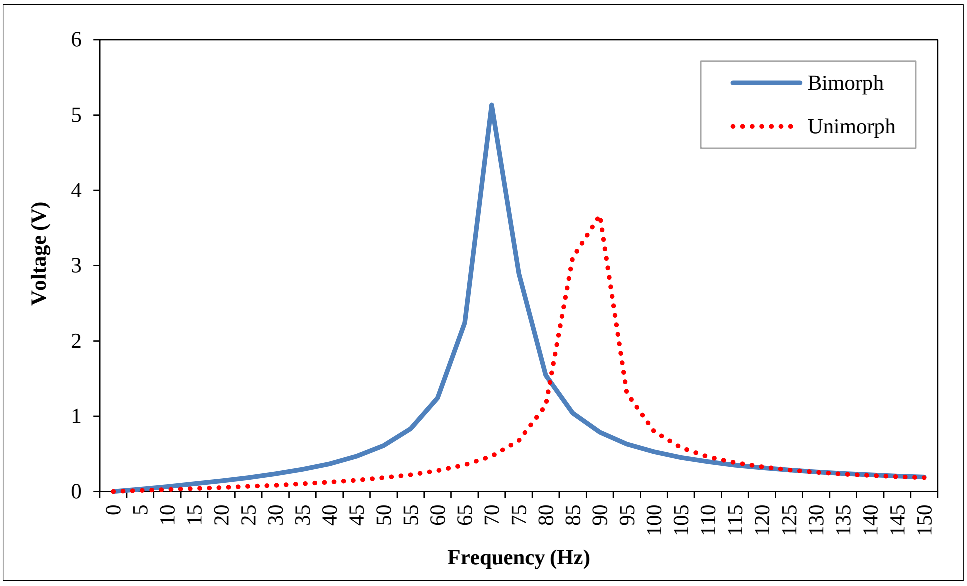

(a)

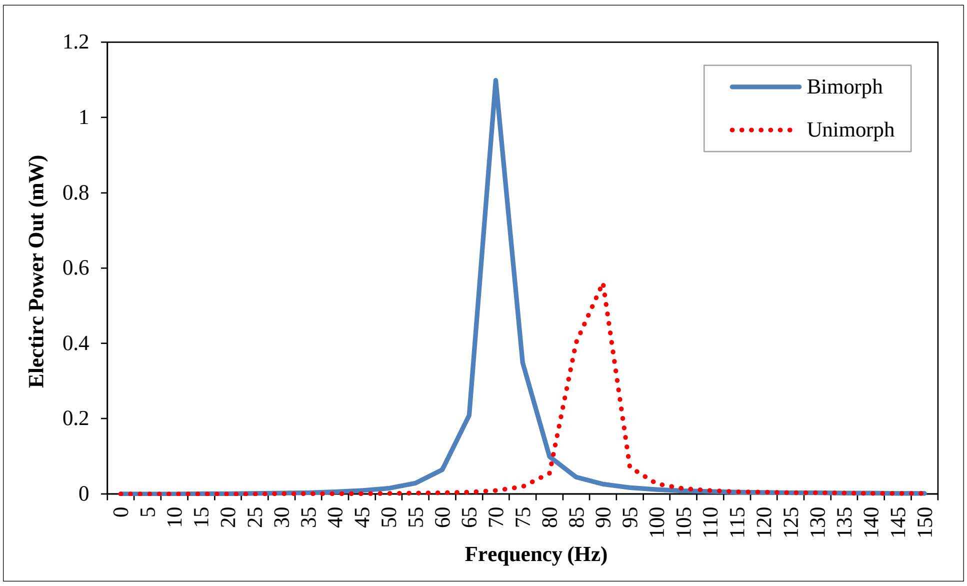

(b)

Figure 5. Bimorph and unimorph cantilever beam (a) Voltage output (b) Electrical output

In Figure 5-b, the bimorph beam again demonstrates superior performance. The peak power output of the bimorph beam reaches 1.098 mW at 70 Hz, while the unimorph beam peaks at 0.56 mW at 90 Hz. Although the power output graph shows a narrower frequency bandwidth compared to the voltage output graph, the bimorph beam still exhibits a broader and more effective frequency range than the unimorph beam. This performance can be attributed to the additional piezoelectric layer in the bimorph structure, which enhances its energy conversion efficiency.

The results demonstrate the superiority of bimorph cantilever beams over unimorph cantilever beams under comparable conditions. Specifically, the bimorph structure achieved a voltage output 39.78% higher and an electrical output 96.07% greater than the unimorph structure. The bimorph cantilever beams, with their additional piezoelectric layer, produced better results without increasing the overall weight of the system. This supports the claim made in [18] that bimorph cantilever beams enhance energy capacity without expanding the unit volume. For both cantilever beam setups of the same dimensions, the unimorph system has a piezoelectric layer thickness of 0.08 mm, while the bimorph configuration has a combined thickness of 0.12 mm. As a result, the output generation capability improved by 39.7%.

The analysis clearly indicates that the bimorph cantilever beam is more effective than the unimorph beam in harvesting energy. The bimorph configuration not only delivers higher voltage and power outputs but also operates effectively over a wider range of frequencies. This makes the bimorph beam more versatile and suitable for applications where varying frequencies are encountered. On the other hand, the unimorph beam, while simpler, is limited in its efficiency and adaptability, as evidenced by its lower output and narrower operational bandwidth. Therefore, for optimal performance in energy harvesting applications, the bimorph cantilever beam is the preferred design choice. The cantilever structure deformed at its first natural frequency of 70.5 Hz. Figure 5 illustrates the displacement of the cantilever beam along with its proof mass. As the second block mass remained fixed, no deformation or displacement was observed.

Figure 6 presents the voltage and electrical power output of a stack cantilever beam as a function of frequency. Figure 6-a indicates that the stack cantilever beam achieves a peak voltage of approximately 4.90 V at a resonant frequency of 158 Hz. Similarly, the electrical power output in Figure 6-b shows a peak power output of about 1 mW at the same resonant frequency of 158 Hz. Figures 6-a and 6-b illustrate a sharp increase in output at the resonant frequency, followed by a rapid decline, highlighting the narrow frequency bandwidth within which the stack cantilever beam operates effectively.

Compared to the bimorph and unimorph cantilever beams shown in Figure 5, the stack cantilever beam displays a significantly higher resonant frequency. While the peak voltage and power outputs are similar in magnitude to those of the bimorph beam, the stack beam's performance is concentrated within a much narrower frequency range. This narrow bandwidth implies that the stack cantilever beam is less versatile than the bimorph beam when dealing with varying frequency inputs, as it is tuned to a specific, higher frequency range. Figures 4 and 5 reveal that while the stack cantilever beam can achieve similar peak outputs as the bimorph cantilever beam, its higher operating frequency and narrower bandwidth limit its effectiveness in applications where a broader frequency range is desirable. The bimorph beam, with its broader operational bandwidth and lower resonant frequency, is more adaptable to a variety of real-world conditions where frequencies may fluctuate. Therefore, despite the stack beam's capability to generate high outputs at a specific frequency, the bimorph cantilever beam remains the superior option for energy harvesting applications that require a wider frequency response.

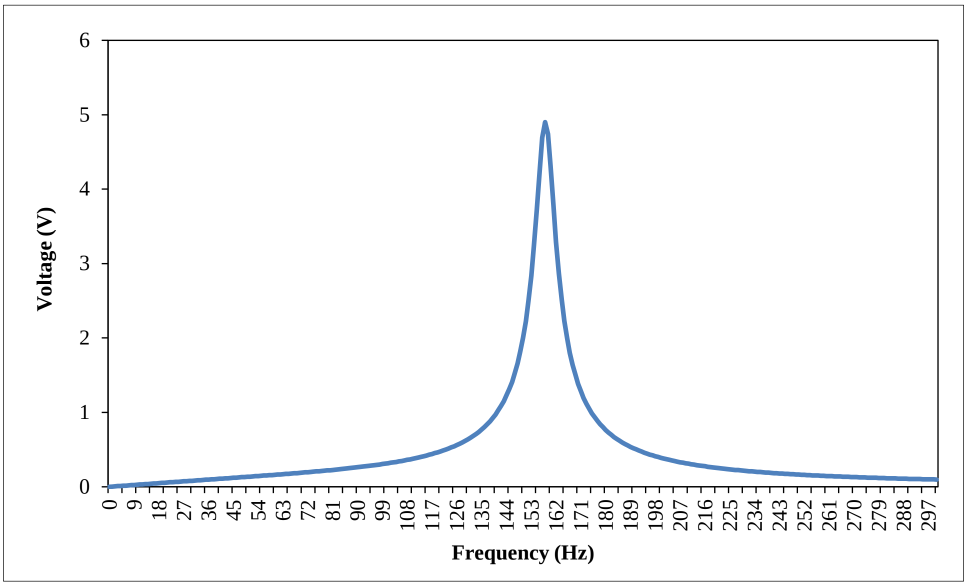

(a)

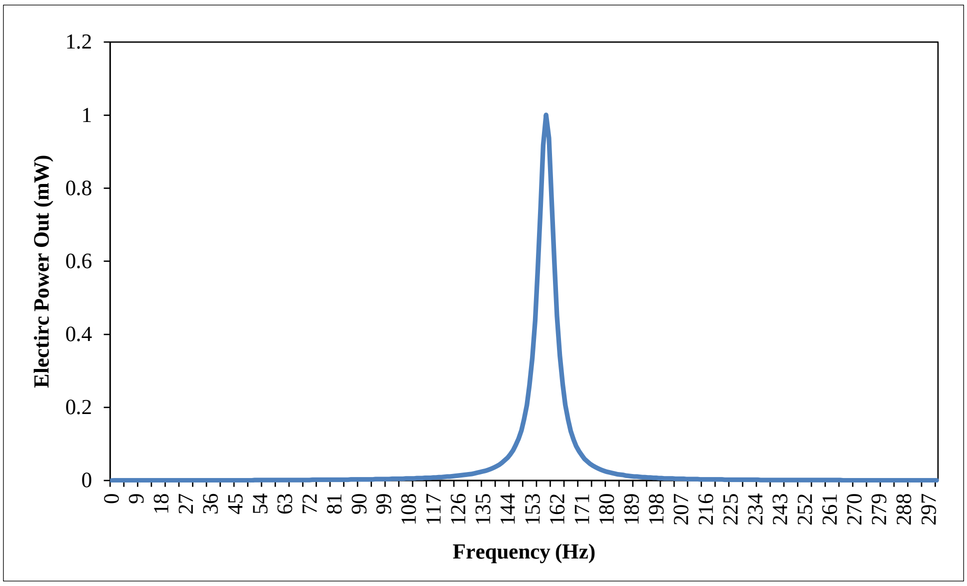

(b)

Figure 6. Stack cantilever beam (a) Voltage output (b) Electrical output tress distribution on the model

While the bimorph configuration yields the highest power output in this study, several potential limitations and trade-offs must be considered when applying this design in practical energy harvesting applications. One key trade-off is the increased complexity and cost of fabrication. A bimorph structure consists of two piezoelectric layers bonded to a substrate, which requires precise alignment and bonding techniques to ensure optimal performance. This adds complexity to the manufacturing process, which could increase production costs compared to simpler unimorph configurations.

Additionally, the bimorph configuration is more sensitive to external mechanical conditions, such as vibration amplitude and frequency. While this sensitivity enables higher energy conversion, it also means that the bimorph may be more prone to mechanical fatigue or failure under continuous or high-stress operating conditions. The increased stiffness in the bimorph structure, which contributes to its higher energy output, could also limit its flexibility in certain applications, particularly where adaptability to varying mechanical loads is required.

Moreover, bimorph designs may exhibit a narrower operational frequency bandwidth, meaning their peak performance is highly dependent on matching the resonant frequency of the device to the application's environmental conditions. This can limit their effectiveness in environments where mechanical vibrations occur at varying or non-resonant frequencies. In contrast, stack or unimorph configurations may offer greater resilience and a broader operational range at the expense of lower power output. Therefore, while the bimorph configuration shows promise for maximizing energy output, these practical considerations must be taken into account when designing energy harvesting systems for real-world applications.

5-3- Types of Piezoelectric Materials

Figure 7 presents a comparative analysis of the voltage output as a function of frequency for two different piezoelectric materials: PZT-5A and PVDF. PZT-5A shows a distinct peak voltage output of approximately 5.13 V at a resonant frequency of 70 Hz. This indicates that PZT-5A is highly efficient at converting mechanical energy into electrical energy at lower frequencies. In contrast, the PVDF material, exhibits a peak voltage output of about 2.64 V, but at a higher resonant frequency of 110 Hz.

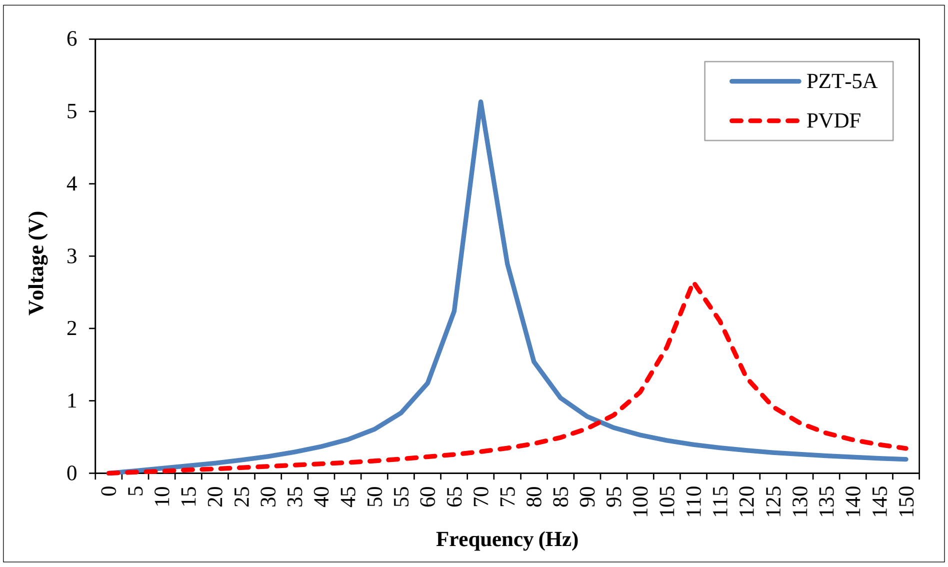

Figure 7. **Voltage output of PZT-5A and PVDF material**

The performance characteristics of these materials reveal several key insights. PZT-5A not only delivers a significantly higher peak voltage output compared to PVDF, but it also does so at a lower frequency, making it particularly suitable for applications where energy harvesting is required at lower vibrational frequencies. The sharp and narrow peak of the PZT-5A curve suggests that its optimal operating range is concentrated around a specific frequency, thereby delivering maximum efficiency within a narrower bandwidth. On the other hand, PVDF, while producing a lower peak voltage output, operates over a broader frequency range. This characteristic can be advantageous in environments where the frequency of vibrations is not constant, as PVDF can accommodate a wider spectrum of frequencies, although at the cost of reduced voltage output efficiency. Although the peak voltage output occurred at a single resonant frequency, considering 20% of the peak performance reveals that PZT-5A maintained 20% of its peak performance from 60 to 85 Hz. In comparison, PVDF, with 20% of its peak voltage (0.528 V), extended its effective performance from 90 to 135 Hz, surpassing the bandwidth of PZT-5A.

Figure 8 illustrates the electrical power output as a function of frequency for two distinct piezoelectric materials: PZT-5A and PVDF. The results reveal a significant contrast in the electrical output capabilities between these two materials, with PZT-5A demonstrating superior performance over PVDF.

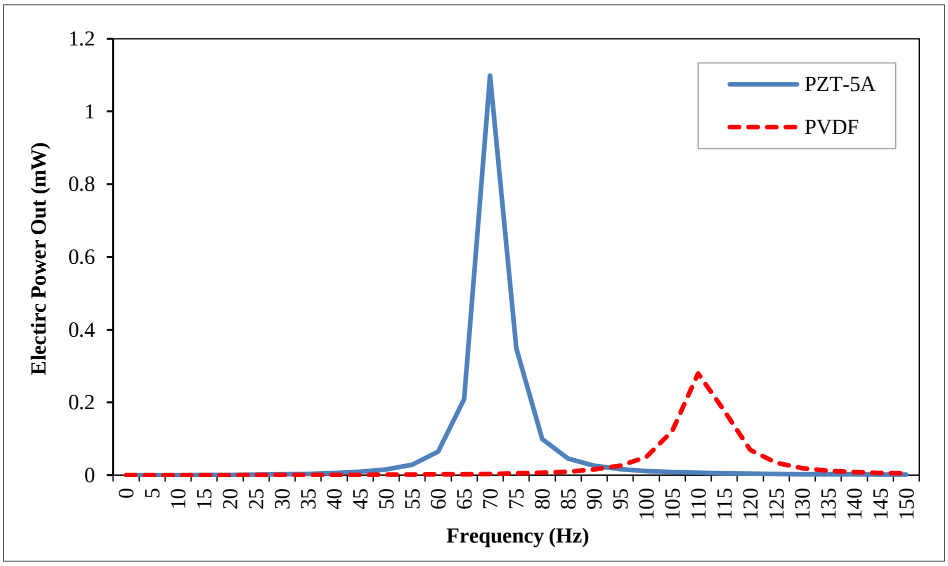

Figure 8. **Electrical output of PZT-5A and PVDF material**

The electrical output of PZT-5A shows a pronounced peak of approximately 1.098 mW at a resonant frequency of 70 Hz. This indicates that PZT-5A is highly effective at converting mechanical vibrations into electrical energy at this specific frequency. The sharpness of the peak suggests that PZT-5A is most efficient within a narrow frequency range, where it can generate maximum electrical power output.

In contrast, the electrical output of PVDF exhibits a lower peak power output of about 0.28 mW at a higher resonant frequency of 110 Hz. Although the peak power output of PVDF is considerably lower than that of PZT-5A, it is important to note that PVDF operates over a broader frequency range. This characteristic can be advantageous in applications where the frequency of ambient vibrations is not constant, allowing PVDF to capture energy across a wider spectrum of frequencies, albeit with lower efficiency. This comparison between organic and inorganic piezoelectric materials supports the assertion in [44] that organic materials like PVDF generally produce lower outputs compared to inorganic materials such as PZT-5A. The higher piezoelectric coefficient of PZT-5A, compared to PVDF, directly results in greater voltage and power output [45].

In Equation 4, where d_{31} represents the piezoelectric coefficient, establishes a direct correlation between the magnitude of the piezoelectric coefficient and the system's voltage response. Since PZT-5A generated nearly double the voltage output of PVDF, it effectively maintained a broader bandwidth frequency with minimum voltage and power response compared to PVDF (0.528 V). The rigidity and stability of PZT materials enable them to endure higher mechanical stress and strain, leading to improved bandwidth [46]. Indeed, PZT-5A's output was 94.32% greater than the peak voltage output of PVDF.

The notable difference in energy conversion efficiency between PZT-5A and PVDF can be attributed to the intrinsic mechanical and electrical properties of the two materials. PZT-5A is a ceramic-based piezoelectric material with a high dielectric constant and piezoelectric coefficient, making it highly responsive to mechanical stress and strain. This translates to a higher energy density and a more efficient conversion of mechanical energy into electrical energy. Its rigid structure and higher Young's modulus enable it to withstand greater mechanical loads, which in turn enhances its ability to generate higher voltage and power outputs, particularly under dynamic conditions such as vibrations.

In contrast, PVDF, an organic polymer-based material, has lower dielectric and piezoelectric constants compared to PZT-5A. While PVDF offers advantages in flexibility, durability, and ease of manufacturing, its lower mechanical stiffness limits its efficiency in energy harvesting applications. The energy conversion in PVDF is less effective because it deforms more easily under mechanical stress, resulting in lower voltage generation and less efficient power output. Additionally, the electrical properties of PVDF, including its relatively lower permittivity, contribute to its reduced performance when compared to PZT-5A. This combination of mechanical and electrical factors explains why PZT-5A outperforms PVDF in energy harvesting applications, particularly in configurations like the bimorph, where maximizing energy conversion is critical.

5-4- Load Resistance Dependence

Figure 9 presents the load resistance dependence of a bimorph cantilever beam utilizing PZT-5A as the piezoelectric material, measured at a fixed resonant frequency of 70 Hz. Figure 9 illustrates three key parameters: voltage (V), mechanical power (mW), and electrical power (mW), each plotted against the load resistance (Ω). The voltage curve shows a steady increase as load resistance rises, eventually reaching a saturation point around 5.5 V at high resistance values (approximately $1E$+5 Ω). This behavior indicates that as load resistance increases, the voltage output of the bimorph cantilever beam continues to grow until it plateaus, suggesting that the system reaches a point where further increases in load resistance do not significantly affect the voltage output. The voltage's late saturation point highlights the efficient energy transfer to the electrical domain in the system, particularly at higher resistance levels.

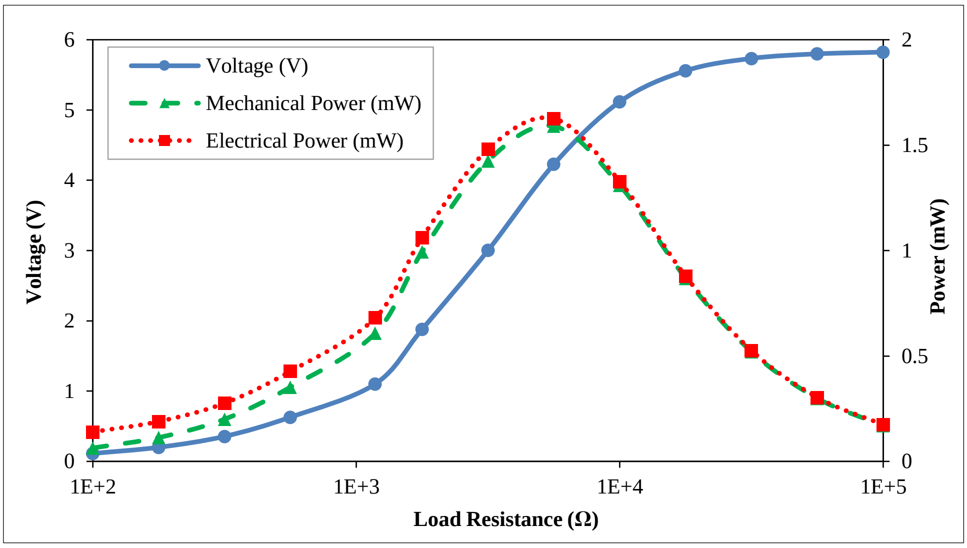

Figure 9. Load Resistance dependence of bimorph cantilever beam with PZT-5A

The mechanical power exhibits a different trend. It initially increases with the load resistance, peaking around (1E+3Ω) before gradually declining. The peak mechanical power output is observed at approximately 1.2 mW, indicating that the system achieves maximum mechanical-to-electrical energy conversion efficiency at this specific load resistance. Beyond this peak, the mechanical power diminishes, suggesting that higher resistance values reduce mechanical energy conversion efficiency.

Similarly, the electrical power output follows a trend similar to that of the mechanical power. It peaks slightly below 1.2 mW at a load resistance of approximately (1E+4Ω) before declining. The peak in electrical power output is crucial for identifying the optimal load resistance to ensure maximum energy harvesting efficiency. The decline in electrical power beyond this peak implies that excessive load resistance leads to a drop in the system's overall energy conversion efficiency.

Figure 9 underscores the complex relationship between load resistance and the output characteristics of a bimorph cantilever beam with PZT-5A. The voltage output continues to rise with increasing load resistance, whereas both mechanical and electrical power outputs exhibit a peak followed by a decline, indicating optimal load resistance ranges for maximizing power output. The analysis suggests a critical load resistance range (between 1E+3Ω and 1E+4Ω) where the system achieves the best balance between voltage generation and power output, essential for designing piezoelectric energy harvesting systems for optimal performance.

Figure 10 illustrates the load resistance dependence of a unimorph cantilever beam with PZT-5A as the piezoelectric material, measured at a fixed resonant frequency of 90 Hz. The voltage curve exhibits a gradual increase as load resistance rises, eventually reaching a maximum value of approximately 1.7 V at high resistance levels (around 1E+5Ω). This trend indicates that as load resistance increases, the voltage output of the unimorph cantilever beam steadily rises without reaching a saturation point within the tested range. The unimorph structure, characterized by its single active piezoelectric layer, inherently generates lower voltage compared to the bimorph structure observed in Figure 8. However, the consistent growth in voltage output suggests that the unimorph beam can still efficiently convert mechanical energy into electrical energy across varying load resistances.

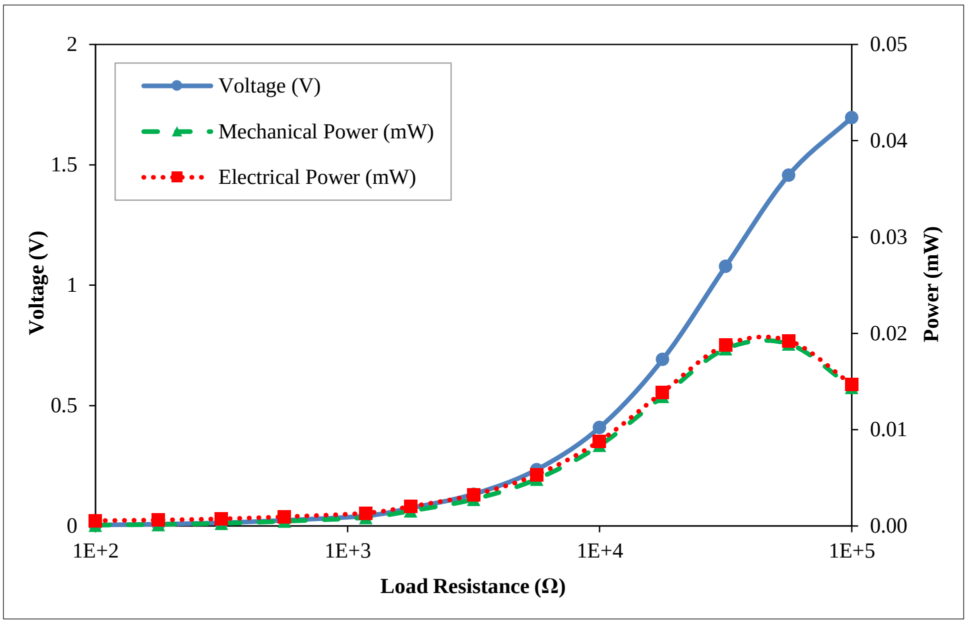

Figure 10. **Load Resistance dependence of unimorph cantilever beam with PZT-5A**

In contrast, the mechanical power output remains relatively low and constant across the entire range of load resistance. It does not exhibit a significant peak, which contrasts with the behavior of the bimorph cantilever beam. This indicates that the unimorph structure is less effective at converting mechanical energy into electrical energy, particularly when load resistance varies. The mechanical power remains below 0.05 mW, suggesting limited mechanical-to-electrical energy conversion efficiency in this configuration.

Similarly, the electrical power output remains low and relatively flat across the entire range of load resistance. It does not display a significant peak and stays below 0.05 mW, further highlighting the limited efficiency of the unimorph cantilever beam in energy harvesting applications. The unimorph beam's single active layer constrains its ability to generate substantial electrical power compared to the bimorph configuration.

Figure 10 highlights the distinct behavior of a unimorph cantilever beam with PZT-5A at a fixed resonant frequency of 90 Hz. The voltage output increases steadily with load resistance, indicating the unimorph's capability to convert mechanical energy into electrical energy, albeit at a lower efficiency than the bimorph structure. Both mechanical and electrical power outputs remain low and relatively constant, suggesting that the unimorph configuration is less effective in energy harvesting applications. This analysis underscores the advantages of bimorph configurations over unimorph structures in maximizing energy conversion efficiency, especially when considering load resistance as a critical factor in optimizing performance.

Figure 11 illustrates the load resistance dependence of PVDF at a fixed resonant frequency of 110 Hz. The voltage curve exhibits a sharp increase with increasing load resistance, showing a nonlinear trend. The voltage remains relatively low and stable across the lower resistance range (10^2 Ω to around 10^4 Ω), but as the resistance exceeds 10^4 Ω, the voltage escalates rapidly, reaching approximately 23 V at the highest resistance of 10^5 Ω. This behavior is indicative of the high impedance nature of PVDF, where voltage output significantly rises with increasing load resistance.

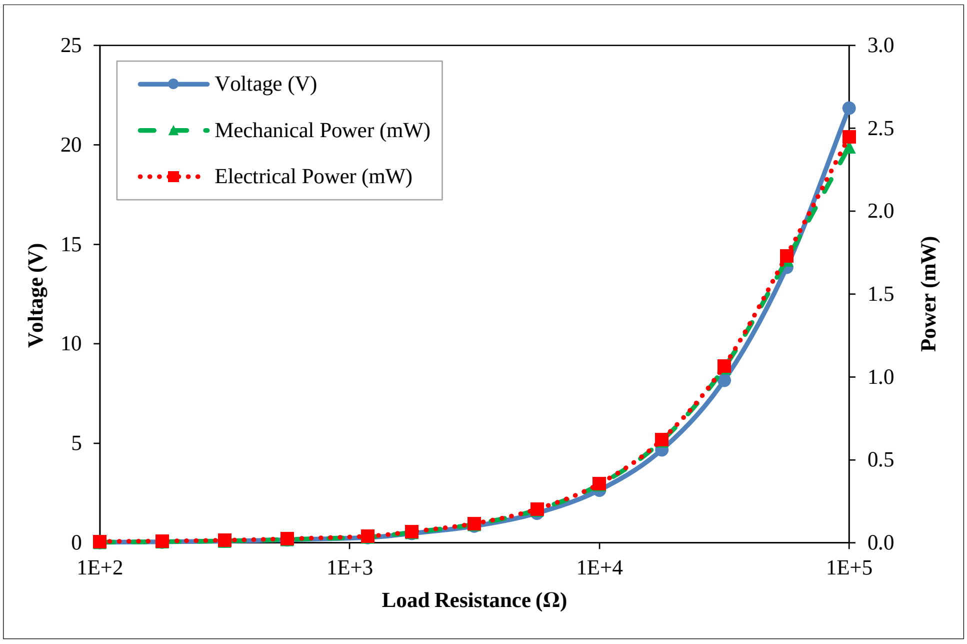

Figure 11. Load resistance dependence of PVDF

On the other hand, both mechanical and electrical power display a more subdued response to changes in load resistance. Across the entire resistance range, these power metrics remain relatively low, with minimal variation, particularly in the lower resistance region. The mechanical power curve suggests that the energy conversion efficiency of the PVDF material remains almost constant, irrespective of the load resistance. The electrical power shows a slight increase as the resistance rises but does not exhibit the same steep climb as the voltage.

Figure 11 demonstrates that while the voltage output of PVDF is highly sensitive to changes in load resistance, peaking at higher resistance values, the associated mechanical and electrical power outputs are largely unaffected, remaining relatively low and stable across the tested resistance range. This suggests that in applications where high voltage output is desired, increasing load resistance may not significantly impact power output in PVDF-based energy harvesting systems.

The findings of this study provide crucial insights for optimizing the design of piezoelectric energy harvesters in practical applications. The bimorph configuration with PZT-5A, which demonstrated superior energy conversion efficiency, can significantly enhance the performance of harvesters used in low-frequency mechanical environments such as structural health monitoring, wearable technology, and wireless sensor networks. In these fields, the optimized configuration could improve the efficiency of sensors and devices that rely on ambient mechanical energy, extending their operational lifespan and reducing maintenance. Specifically, this optimization is beneficial for applications like monitoring infrastructure vibrations, powering wearable devices, and enabling self-sustaining IoT sensors in remote areas. By selecting the appropriate materials and configurations, designers can effectively harness low-frequency vibrations, leading to more efficient and sustainable energy solutions across various industries.

6- Conclusion

This study analyzed the impact of the number of piezoelectric layers and the type of piezoelectric material used in cantilever-based piezoelectric energy harvesters. The findings underscore the significant impact of both material choice and cantilever beam configuration on energy harvesting performance. PZT-5A demonstrated superior energy conversion capabilities compared to PVDF, particularly at resonant frequencies, where it generates up to 94.34% higher voltage output. Among the three configurations tested—unimorph, bimorph, and stack—the bimorph configuration with PZT-5A achieved the highest efficiency, with electrical power output increasing by 50% compared to the unimorph configuration and by 9% over the stack configuration. In contrast, the unimorph cantilever configuration, while still functional, produces lower voltage and power outputs, indicating a 30% reduction in efficiency compared to the bimorph structure. The stack configuration, although better than the unimorph, falls short by 8% in electrical power output compared to the bimorph. These results suggest that for applications where high energy conversion efficiency is crucial, the use of PZT-5A in a bimorph configuration is particularly advantageous. This study provides valuable insights for optimizing the design of piezoelectric energy harvesting systems, paving the way for more effective and efficient deployment across various technological applications.

7- Nomenclature

A	Effective area of the piezoelectric layer, m^2	A_p	Area of the piezoelectric element, m^2
A_s	Area of the substrate element, m^2	C	Capacitance, F
c	Damping coefficient	d	Separation distance between the piezoelectric layer and the opposing electrode, m
d_{31}	Piezoelectric strain constant	E	Young's modulus, Pa
f	Frequency of mechanical excitation, Hz	F_p	Applied excitation force, N
F_e	Electromechanical force, N	g	Piezoelectric voltage constant
I	Moment of inertia, kg·m^2	k	Beam's stiffness coefficient
k_t	Stiffness of the tip mass, N/m	m	Total mass of the beam, kg
P	Electrical power, mW	t	Time, sec
V	Voltage output, V	w	Vertical displacement of the beam, m
w_t	Displacement of the tip mass, m	x	Axial position along the beam
ε_0	Vacuum permittivity (Aprrox. 8.854×10^{-12} F/m)	ε_r	Relative permittivity
$\varepsilon_{r,p}$	Relative permittivity of the piezoelectric material	$\varepsilon_{r,s}$	Relative permittivity of the substrate material
Δp	Mechanical strain induced in the piezoelectric material, C/N		

8- Declarations

8-1- Author Contributions

Conceptualization, F.H.S., L.W.T., and M.F.B.; methodology, F.H.S. and L.W.T.; software, F.H.S.; validation, F.H.S.; formal analysis, F.H.S., L.W.T., and M.F.B.; investigation, F.H.S.; resources, F.H.S. and L.W.T.; data curation, F.H.S.; writing—original draft preparation, F.H.S. and M.F.B.; writing—review and editing, L.W.T.; visualization, F.H.S. and L.W.T.; supervision, L.W.T.; project administration, L.W.T., Y.K.C., and M.N.E.E.; funding acquisition, L.W.T. All authors have read and agreed to the published version of the manuscript.

8-2- Data Availability Statement

The data presented in this study are available on request from the corresponding author.

8-3- Funding and Acknowledgments

This work was supported by the Ministry of Higher Education of Malaysia under the Fundamental Research Grant Scheme (FRGS/1/2020/TK0/MMU/03/13). The authors would also like to acknowledge the Faculty of Engineering and Technology, Multimedia University for the support given in conducting this research.

8-4- Institutional Review Board Statement

Not applicable.

8-5- Informed Consent Statement

Not applicable.

8-6- Conflicts of Interest

The authors declare that there is no conflict of interest regarding the publication of this manuscript. In addition, the ethical issues, including plagiarism, informed consent, misconduct, data fabrication and/or falsification, double publication and/or submission, and redundancies have been completely observed by the authors.

9- References

[1] Wu, Y., Ma, Y., Zheng, H., & Ramakrishna, S. (2021). Piezoelectric materials for flexible and wearable electronics: A review. Materials & Design, 211. doi:10.1016/j.matdes.2021.110164.

[2] Ali, F., Raza, W., Li, X., Gul, H., & Kim, K. H. (2019). Piezoelectric energy harvesters for biomedical applications. Nano Energy, 57, 879–902. doi:10.1016/j.nanoen.2019.01.012.

[3] Cheng, X., Xue, X., Ma, Y., Han, M., Zhang, W., Xu, Z., Zhang, H., & Zhang, H. (2016). Implantable and self-powered blood pressure monitoring based on a piezoelectric thin film: Simulated, in vitro and in vivo studies. Nano Energy, 22, 453–460. doi:10.1016/j.nanoen.2016.02.037.

[4] Grossi, M. (2021). Energy harvesting strategies for wireless sensor networks and mobile devices: A review. Electronics (Switzerland), 10(6), 1–53. doi:10.3390/electronics10060661.

[5] Le Scornec, J., Guiffard, B., Seveno, R., Le Cam, V., & Ginestar, S. (2022). Self-powered communicating wireless sensor with flexible aero-piezoelectric energy harvester. Renewable Energy, 184, 551–563. doi:10.1016/j.renene.2021.11.113.

[6] Pertin, O., Guha, K., Jakšić, O., Jakšić, Z., & Iannacci, J. (2022). Investigation of Nonlinear Piezoelectric Energy Harvester for Low-Frequency and Wideband Applications. Micromachines, 13(9), 1399. doi:10.3390/mi13091399.

[7] Yang, S., Cui, X., Guo, R., Zhang, Z., Sang, S., & Zhang, H. (2020). Piezoelectric sensor based on graphene-doped PVDF nanofibers for sign language translation. Beilstein Journal of Nanotechnology, 11, 1655–1662. doi:10.3762/BJNANO.11.148.

[8] Liu, Y., Khanbareh, H., Halim, M. A., Feeney, A., Zhang, X., Heidari, H., & Ghannam, R. (2021). Piezoelectric energy harvesting for self- powered wearable upper limb applications. Nano Select, 2(8), 1459–1479. doi:10.1002/nano.202000242.

[9] Gilson Dranka, G., Ferreira, P., & Vaz, A. I. F. (2022). Co-benefits between energy efficiency and demand-response on renewable-based energy systems. Renewable and Sustainable Energy Reviews, 169. doi:10.1016/j.rser.2022.112936.

[10] Ang, T. Z., Salem, M., Kamarol, M., Das, H. S., Nazari, M. A., & Prabaharan, N. (2022). A comprehensive study of renewable energy sources: Classifications, challenges and suggestions. Energy Strategy Reviews, 43, 100939. doi:10.1016/j.esr.2022.100939.

[11] Santika, W. G., Anisuzzaman, M., Bahri, P. A., Shafiullah, G. M., Rupf, G. V., & Urmee, T. (2019). From goals to joules: A quantitative approach of interlinkages between energy and the Sustainable Development Goals. Energy Research and Social Science, 50, 201–214. doi:10.1016/j.erss.2018.11.016.

[12] Seung Choi, H., Hur, S., Kumar, A., Song, H., Min Baik, J., Song, H. C., & Ryu, J. (2023). Continuous pyroelectric energy generation with cyclic magnetic phase transition for low-grade thermal energy harvesting. Applied Energy, 344, 121271. doi:10.1016/j.apenergy.2023.121271.

[13] Anand, A., Ghose, D., Pradhan, S., Shabbiruddin, Bhoi, A.K. (2020). Optimal Selection of Electric Motor for E-Rickshaw Application Using MCDM Tools. Cognitive Informatics and Soft Computing. Advances in Intelligent Systems and Computing, vol 1040. Springer, Singapore. doi:10.1007/978-981-15-1451-7_52.

[14] Saadon, S., & Sidek, O. (2011). A review of vibration-based MEMS piezoelectric energy harvesters. Energy Conversion and Management, 52(1), 500–504. doi:10.1016/j.enconman.2010.07.024.

[15] Shindo, Y., & Narita, F. (2014). Dynamic bending/torsion and output power of S-shaped piezoelectric energy harvesters. International Journal of Mechanics and Materials in Design, 10(3), 305–311. doi:10.1007/s10999-014-9247-0.

[16] Zhou, W., Penamalli, G. R., & Zuo, L. (2012). An efficient vibration energy harvester with a multi-mode dynamic magnifier. Smart Materials and Structures, 21(1). doi:10.1088/0964-1726/21/1/015014.

[17] Shin, Y. H., Choi, J., Kim, S. J., Kim, S., Maurya, D., Sung, T. H., Priya, S., Kang, C. Y., & Song, H. C. (2020). Automatic resonance tuning mechanism for ultra-wide bandwidth mechanical energy harvesting. Nano Energy, 77. doi:10.1016/j.nanoen.2020.104986.

[18] Krishna, A., & Palanivelu, S. (2023). Energy Harvesting from Vibrating Cantilever Structure of Different Base Materials using Piezoelectric Material: Theoretical and Experimental Approach. International Journal of Engineering, Transactions A: Basics, 36(1), 152–162. doi:10.5829/ije.2023.36.01a.17.

[19] Karim H. Ali, Ahmed alhamadani, & Thaier J. Ntayeesh. (2024). Design and optimization of piezoelectric energy harvesting systems for enhanced performance in wireless sensor networks. International Journal of Science and Research Archive, 12(2), 568–576. doi:10.30574/ijsra.2024.12.2.1079.

[20] Khan, A., Nawaz, M. Q., & Xu, L. (2024). Investigation and Numerical Simulation of Different Piezoelectric Bimorph Cantilever Designs for Energy Harvesting. International Journal of Electrical, Energy and Power System Engineering, 7(2), 85–99. doi:10.31258/ijeepse.7.2.85-99.

[21] Megdich, A., Habibi, M., Laperrière, L., Li, Z., & Abdin, Y. (2024). Enhanced piezoelectric performance of PVDF/MWCNTs energy harvester through a 3D-printed multimodal auxetic structure for smart security systems. Materials Today Sustainability, 27, 100847. doi:10.1016/j.mtsust.2024.100847.

[22] Al Miraj, A., Uddin, A. M., Gani, M. M., Sultana, T., & Shultana, S. (2024). Performance Analysis of Different Piezoelectric & Shim Materials on Bimorph Piezoelectric Energy Harvester. 2024 IEEE 9th International Conference for Convergence in Technology, I2CT 2024. doi:10.1109/I2CT61223.2024.10543375.

[23] Xi, K., Hou, Y., Zheng, M., & Zhu, M. (2024). Elastic Polarization Configuration Coupled with Activity Rattling Space Boosts Energy Harvesting Performance of Lead-Free Piezoceramic. Advanced Functional Materials, 34(29), 2401487. doi:10.1002/adfm.202401487.

[24] Machu, Z., Rubes, O., Sevecek, O., & Hadas, Z. (2021). Experimentally verified analytical models of piezoelectric cantilevers in different design configurations. Sensors, 21(20), 6759. doi:10.3390/s21206759.

[25] He, Q., & Briscoe, J. (2024). Piezoelectric Energy Harvester Technologies: Synthesis, Mechanisms, and Multifunctional Applications. ACS Applied Materials and Interfaces, 16(23), 29491–29520. doi:10.1021/acsami.3c17037.

[26] Al Anazi, A. A., Candra, O., Chammam, A., Marhoon, H. A., Ali, I. R., Al-Kharsan, I. H., Alayi, R., Ebazadeh, Y., & Aladdin, M. (2023). Modeling and investigating electric power output maximization for piezoelectric energy harvester. AIP Advances, 13(5), 0141848. doi:10.1063/5.0141848.

[27] Erturk, A., & Inman, D. J. (2009). An experimentally validated bimorph cantilever model for piezoelectric energy harvesting from base excitations. Smart Materials and Structures, 18(2), 025009. doi:10.1088/0964-1726/18/2/025009.

[28] Kim, M., Hoegen, M., Dugundji, J., & Wardle, B. L. (2010). Modeling and experimental verification of proof mass effects on vibration energy harvester performance. Smart Materials and Structures, 19(4), 045023. doi:10.1088/0964-1726/19/4/045023.

[29] Li, M., Yu, D., Li, Y., Liu, X., & Dai, F. (2023). Integrated a nonlinear energy sink and a piezoelectric energy harvester using simply-supported bi-stable piezoelectric composite laminate. International Journal of Non-Linear Mechanics, 156. doi:10.1016/j.ijnonlinmec.2023.104464.

[30] Tang, L., & Wang, J. (2017). Size effect of tip mass on performance of cantilevered piezoelectric energy harvester with a dynamic magnifier. Acta Mechanica, 228(11), 3997–4015. doi:10.1007/s00707-017-1910-8.

[31] Syed, F. H., Thong, L. W., & Chan, Y. K. (2023). Analysis of Piezoelectric Energy Harvester with Different Substrate Materials and Configurations. Proceedings of the Multimedia University Engineering Conference (MECON 2022), 297–314. doi:10.2991/978-94-6463-082-4_27.

[32] Ali, A., Shaukat, H., Bibi, S., Altabey, W. A., Noori, M., & Kouritem, S. A. (2023). Recent progress in energy harvesting systems for wearable technology. Energy Strategy Reviews, 49. doi:10.1016/j.esr.2023.101124.

[33] Mo, X., Zhou, H., Li, W., Xu, Z., Duan, J., Huang, L., Hu, B., & Zhou, J. (2019). Piezoelectrets for wearable energy harvesters and sensors. Nano Energy, 65. doi:10.1016/j.nanoen.2019.104033.

[34] Takahashi, H., Numamoto, Y., Tani, J., Matsuta, K., Qiu, J., & Tsurekawa, S. (2005). Lead-Free Barium Titanate Ceramics with Large Piezoelectric Constant Fabricated by Microwave Sintering. Japanese Journal of Applied Physics, 45(1L), L30. doi:10.1143/jjap.45.l30.

[35] Hao, J., Li, W., Zhai, J., & Chen, H. (2019). Progress in high-strain perovskite piezoelectric ceramics. Materials Science and Engineering R: Reports, 135, 1–57. doi:10.1016/j.mser.2018.08.001.

[36] Karaki, T., Yan, K., Miyamoto, T., & Adachi, M. (2007). Lead-Free Piezoelectric Ceramics with Large Dielectric and Piezoelectric Constants Manufactured from BaTiO3 Nano-Powder. Japanese Journal of Applied Physics, 46(2L), L97. doi:10.1143/jjap.46.l97.

[37] Anton, S. R., & Sodano, H. A. (2007). A review of power harvesting using piezoelectric materials (2003-2006). Smart Materials and Structures, 16(3), R01. doi:10.1088/0964-1726/16/3/R01.

[38] Lang, S. B., & Muensit, S. (2006). Review of some lesser-known applications of piezoelectric and pyroelectric polymers. Applied Physics A, 85(2), 125–134. doi:10.1007/s00339-006-3688-8.

[39] Fu, J., Hou, Y., Gao, X., Zheng, M., & Zhu, M. (2018). Highly durable piezoelectric energy harvester based on a PVDF flexible nanocomposite filled with oriented BaTi2O5 nanorods with high power density. Nano Energy, 52, 391–401. doi:10.1016/j.nanoen.2018.08.006.

[40] Yang, L., Chi, S., Dong, S., Yuan, F., Wang, Z., Lei, J., Bao, L., Xiang, J., & Wang, J. (2020). Preparation and characterization of a novel piezoelectric nanogenerator based on soluble and meltable copolyimide for harvesting mechanical energy. Nano Energy, 67, 104220. doi:10.1016/j.nanoen.2019.104220.

[41] Ghosh, S. K., Sinha, T. K., Mahanty, B., & Mandal, D. (2015). Self-poled Efficient Flexible "Ferroelectretic" Nanogenerator: A New Class of Piezoelectric Energy Harvester. Energy Technology, 3(12), 1190–1197. doi:10.1002/ente.201500167.

[42] Syed, F. H., Thong, L. W., & Chan, Y. K. (2023). Evaluation of Substrate Materials and Mass Structure on Piezoelectric Cantilever Based Energy Harvester. Journal of Engineering Science and Technology, 18(6), 3140-3154.

[43] Comsol (2025). MEMS Module Application Library: COMSOL Trademarks, Burlington, Canada. Available online: www.comsol.com/trademarks (accessed on January 2025).

[44] Liu, H., Zhong, J., Lee, C., Lee, S. W., & Lin, L. (2018). A comprehensive review on piezoelectric energy harvesting technology: Materials, mechanisms, and applications. Applied Physics Reviews, 5(4), 041306. doi:10.1063/1.5074184.

[45] Jain, A., K. J., P., Sharma, A. Kr., Jain, A., & P.N, R. (2015). Dielectric and piezoelectric properties of PVDF/PZT composites: A review. Polymer Engineering & Science, 55(7), 1589–1616. doi:10.1002/pen.24088.

[46] Pei, J., Zhao, Z., Li, X., Liu, H., & Li, R. (2017). Effect of preparation techniques on structural and electrical properties of PZT/PVDF composites. Materials Express, 7(3), 180–188. doi:10.1166/mex.2017.1369.